STRUCTURAL CHEMISTRY

ISSN: 2053-2296
journals.iucr.org/c

The antitumour drug 7-ethyl-10-hydroxycamptothecin monohydrate and its solid-state hydrolysis mechanism on heating

Md. Ashraf Ali, Shuji Noguchi, Miteki Watanabe, Yasunori Iwao and Shigeru Itai

Acta Cryst. (2016). C**72**, 743–747

STRUCTURAL CHEMISTRY
ISSN 2053-2296

The antitumour drug 7-ethyl-10-hydroxycamptothecin monohydrate and its solid-state hydrolysis mechanism on heating

Md. Ashraf Ali,[a,b] Shuji Noguchi,[c,d] Miteki Watanabe,[c] Yasunori Iwao[c] and Shigeru Itai[c]*

[a]Graduate School of Integrated Pharmaceutical and Nutritional Sciences, University of Shizuoka, 52-1 Yada, Suruga-ku, Shizuoka 422-8526, Japan, [b]Department of Pharmacy, Faculty of Life Science, Mawlana Bhashani Science and Technology University, Santosh, Tangail-1902, Bangladesh, [c]School of Pharmaceutical Sciences, University of Shizuoka, 52-1 Yada, Suruga-ku, Shizuoka 422-8526, Japan, and [d]Faculty of Pharmaceutical Sciences, Toho University, 2-2-1 Miyama, Funabashi City, Chiba 274-8510, Japan. *Correspondence e-mail: s-itai@u-shizuoka-ken.ac.jp

Received 7 July 2016
Accepted 13 September 2016

Edited by Y. Ohgo, Teikyo University, Japan

Keywords: 7-ethyl-10-hydroxycamptothecin; antitumour drugs; topoisomerase I inhibitor; solid-state hydrolysis; crystal structure; anticancer agent; irinotecan; synchrotron.

CCDC reference: 1504071

Supporting information: this article has supporting information at journals.iucr.org/c

7-Ethyl-10-hydroxycamptothecin [systematic name: (4*S*)-4,11-diethyl-4,9-dihydroxy-1*H*-pyrano[3′,4′:6,7]indolizino[1,2-*b*]quinoline-3,14(4*H*,12*H*)-dione, SN-38] is an antitumour drug which exerts activity through the inhibition of topoisomerase I. The crystal structure of SN-38 as the monohydrate, $C_{22}H_{20}N_2O_5\cdot H_2O$, reveals that it is a monoclinic crystal, with one SN-38 molecule and one water molecule in the asymmetric unit. When the crystal is heated to 473 K, approximately 30% of SN-38 is hydrolyzed at its lactone ring, resulting in the formation of the inactive carboxylate form. The molecular arrangement around the water molecule and the lactone ring of SN-38 in the crystal structure suggests that SN-38 is hydrolyzed by the water molecule at (x, y, z) nucleophilically attacking the carbonyl C atom of the lactone ring at ($x-1$, y, $z-1$). Hydrogen bonding around the water molecules and the lactone ring appears to promote this hydrolysis reaction: two carbonyl O atoms, which are hydrogen bonded as hydrogen-bond acceptors to the water molecule at (x, y, z), might enhance the nucleophilicity of this water molecule, while the water molecule at ($-x$, $y+\frac{1}{2}$, $-z$), which is hydrogen bonded as a hydrogen-bond donor to the carbonyl O atom at ($x-1$, y, $z-1$), might enhance the electrophilicity of the carbonyl C atom.

1. Introduction

7-Ethyl-10-hydroxycamptothecin [systematic name: (4*S*)-4,11-diethyl-4,9-dihydroxy-1*H*-pyrano[3′,4′:6,7]indolizino[1,2-*b*]-quinoline-3,14(4*H*,12*H*)-dione, SN-38] is an active metabolite of the prodrug irinotecan. SN-38 is an effective anticancer agent, which induces cell death by inhibiting the nuclear enzyme topoisomerase I during DNA replication and transcription (Pommier, 2006). Although the prodrug irinotecan has been used widely for the treatment of colorectal cancer and many other solid tumours (Potmesil, 1994), it has been reported that only 2–8% of an injected dose of irinotecan in humans was converted into active SN-38 (Rothenberg *et al.*, 2001). SN-38 has been reported to show a 10^2- to 10^3-fold more potent cytotoxicity *in vitro* compared with irinotecan (Chabot, 1997). Various types of formulations and drug-delivery systems have been investigated for the formulation of SN-38 to improve its applicability by increasing water solubility, bioavailability and stability. Examples include chemical modification using polymers (Sapra *et al.*, 2008; Kolhatkar *et al.*, 2008), and nanoparticle formulations such as liposomes (Zhang *et al.*, 2004), micelles (Hamaguchi *et al.*, 2010), poly

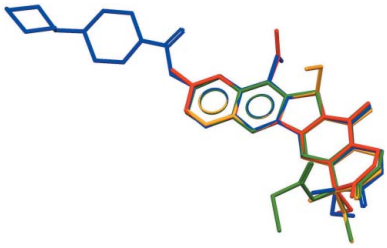

lactic-co-glycolic acid nanoparticles (Sepehri *et al.*, 2014) and cubosomes (Ali *et al.*, 2016). SN-38 exists in solution in an equilibrium between the lactone form and the hydrolyzed carboxylate form, which is inactive (Thakur *et al.*, 2010). Although the crystal structure of irinotecan has been determined using single-crystal X-ray diffraction [Cambridge Structural Database (CSD; Groom & Allen, 2014) entry VOGCAV; Sawada *et al.*, 1991], that of SN-38 has not yet been reported. In this work, we have determined the single-crystal structure of SN-38 monohydrate, (I), and have also investigated its solid-state hydrolysis on heating.

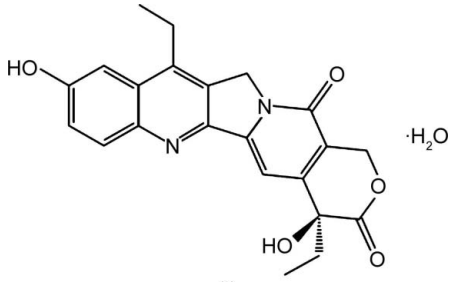

(I)

2. Experimental

2.1. Crystallization

SN-38 was purchased from Tokyo Chemical Industry Co., Ltd (Tokyo, Japan). All other reagents used in this study were of the highest grade commercially available. SN-38 was dissolved in acetone, and the acetone solution was centrifuged at 10 000 *g* for 10 min. The supernatant (approximately 1 ml) was poured into a Petri dish and allowed to evaporate slowly at room temperature. Fine transparent crystals of (I) with a columnar shape had grown within 1 d. The powder X-ray diffraction (PXRD) pattern of the recrystallized crystals measured using a Mini Flex II (Rigaku Corporation, Tokyo, Japan) diffractometer was identical to that of the SN-38 crystals purchased from Tokyo Chemical Industry. This ensured that the crystal forms were the same before and after the recrystallization process. Interestingly, the supplied material is not labelled as the monohydrate, even though our experiments showed that the newly purchased unopened reagent was pure monohydrate.

2.2. Refinement

Crystal data, data collection and structure refinement results are summarized in Table 1. All H atoms, including those in the water molecule, were located in a difference Fourier map. The positions of the water H atoms were refined with O—H and H···H distance restraints of 0.84 (1) and 1.34 (1) Å, respectively. All other H atoms were placed in idealized positions and constrained to ride on their parent atoms, with C—H = 0.95–0.99 Å and O—H = 0.84 Å. For all H atoms, U_{iso}(H) = 1.2U_{eq}(C,O).

2.3. PXRD measurement on heating

Fine crystal powders of SN-38 were prepared using a pestle and mortar. The ground crystal powders were packed into Lindemann glass capillaries of 0.3 mm diameter and used for a PXRD study of the effect of heating. PXRD data were collected on beamline BL5S2 at the Aichi Synchrotron Radiation Center, which was equipped with a Debye–Sherrer camera and a Pilatus 100K area detector (Rigaku, Tokyo, Japan). The distance between the detector and the sample was set to 340 mm and the detector was tilted by $2\theta = 9^\circ$, so that powder diffractions with 2θ values of up to 16° could be recorded. The wavelength was set to 1.000 Å. During data collection, the samples were rotated at 3.3 r min^{-1} to minimize the effect of preferential orientation. The samples were heated from 298 to 573 K at a rate of 10 K min^{-1} using an N_2 gas flow. PXRD data were recorded sequentially with an exposure time of 18 s. The amount of crystals upon heating was estimated using the integrated intensities, $I(T)$, of the diffraction peaks at temperature T, and changes were analysed by plotting the ratio $I(T)/I_{max}$, where I_{max} is the maximum value of $I(T)$. The peak used for the plot was that at a 2θ value of around 7.2° [$(\bar{1}01)$] in the case of the SN-38·H_2O crystals, while that at a 2θ value of around 10.1° was used in the case of the crystal form which emerged on heating.

Table 1
Experimental details.

Crystal data	
Chemical formula	$C_{22}H_{20}N_2O_5·H_2O$
M_r	410.42
Crystal system, space group	Monoclinic, $P2_1$
Temperature (K)	100
a, b, c (Å)	8.529 (2), 7.352 (2), 15.075 (3)
β (°)	100.18 (3)
V (Å^3)	930.3 (4)
Z	2
Radiation type	Synchrotron (SPring-8 BL02B1), λ = 0.70041 Å
μ (mm^{-1})	0.11
Crystal size (mm)	0.20 × 0.01 × 0.01
Data collection	
Diffractometer	Rigaku Mercury2 four-circle diffractometer with CCD area detector
No. of measured, independent and observed [$I > 2\sigma(I)$] reflections	13173, 4345, 3684
R_{int}	0.056
(sin $\theta/\lambda)_{max}$ (Å^{-1})	0.685
Refinement	
$R[F^2 > 2\sigma(F^2)]$, $wR(F^2)$, S	0.043, 0.120, 0.84
No. of reflections	4345
No. of parameters	281
No. of restraints	16
H-atom treatment	H atoms treated by a mixture of independent and constrained refinement
$\Delta\rho_{max}$, $\Delta\rho_{min}$ (e Å^{-3})	0.42, −0.28

Computer programs: *RAPID-AUTO* (Rigaku, 1999), *SHELXT* (Sheldrick, 2015*a*), *SHELXL2014* (Sheldrick, 2015*b*), *SHELXLE* (Hübschle *et al.*, 2011), *Mercury* (Macrae *et al.*, 2008) and *publCIF* (Westrip, 2010).

2.4. High-performance liquid chromatography (HPLC) analyses

After heating to 473 K for 10 min, the SN-38·H_2O samples were dissolved in acetonitrile and analysed using HPLC to

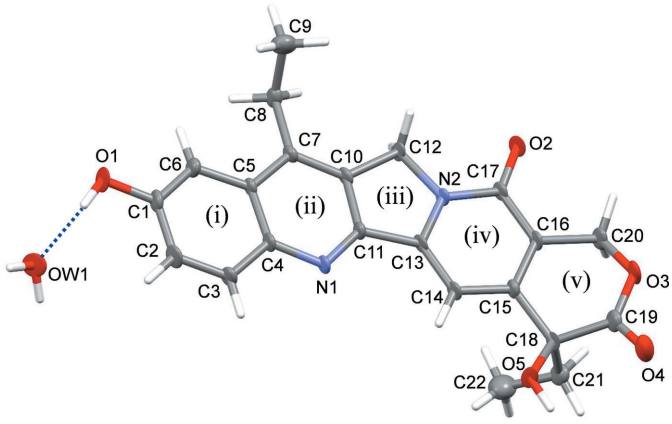

Figure 1
The molecular structure of SN-38 monohydrate and the atom-numbering scheme used. C, H, O and N atoms are shown in grey, white, red and pale violet, respectively. Displacement ellipsoids are drawn at the 75% probability level. Roman numerals in parentheses indicate the ring-numbering system used. The hydrogen bond between SN-38 and the water molecule is shown as a blue dotted line.

identify the products on heating, under the conditions described previously (Ali *et al.*, 2016). A TSKgel ODS-80Tm column was employed and the mobile phase used was a 1:1 (*v*/*v*) mixture of acetonitrile and 25 m*M* sodium phosphate buffer (pH 7.4). SN-38 and degradation products on heating were detected with a UV absorption spectrometer set at a wavelength of 265 nm.

3. Results and discussion

The refined crystal structure reveals that the asymmetric unit of (I) consists of one SN-38 molecule and one water molecule (Fig. 1), indicating that the crystal is SN-38 monohydrate. The water molecule may be a by-product generated during the SN-38 synthesis (Latinen, 2006). Rings (i), (ii), (iii) and (iv) of SN-38 (defined in Fig. 1) are almost coplanar but slightly curved, and the angle formed by the best-fit planes of rings (i) and (iv) is 6.89 (14)°. When the aromatic rings (i), (ii) and (iii) of SN-38 are superimposed on those of irinotecan, camptothecin iodoacetate (CSD entry CAMPTC10; McPhail & Sim, 1968) and 5β-(hydroxymethyl)camptothecin (CSD entry YIZYEL; Wang *et al.*, 1995), a difference in conformation is found at the lactone rings (Fig. 2). All the lactone rings of these compounds adopt a boat conformation, as is often observed in the six-membered lactone rings of multicyclic compounds (Dai *et al.*, 2010; Jenkinson *et al.*, 2010). The C15—C16—C20—O3 torsion angle in SN-38, which indicates the planarity of the six-membered lactone ring, is −30.0 (4)°, while those of irinotecan, camptothecin iodoacetate and 5β-hydroxymethyl camptothecin are −14 (2), −33.3 and −24.9°, respectively. This shows that the lactone rings of SN-38, camptothecin iodoacetate and 5β-(hydroxymethyl)camptothecin are less planar than that of irinotecan. This variation in conformation might suggest conformational flexibility of the lactone rings in the camptothecin skeleton.

In the crystal structure of (I), aromatic rings (i)–(iv) of SN-38 are nearly parallel to the *ac* plane and are stacked along

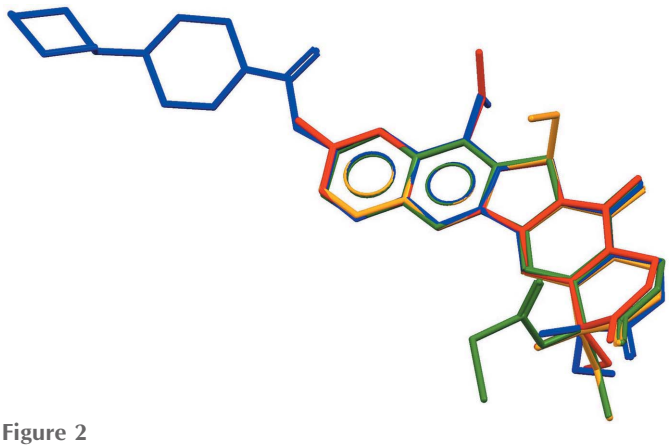

Figure 2
Superposition of the molecular structures of SN-38 (red), irinotecan (blue), camptothecin iodoacetate (green) and 5β-(hydroxymethyl)-camptothecin (orange). H atoms have been omitted for clarity.

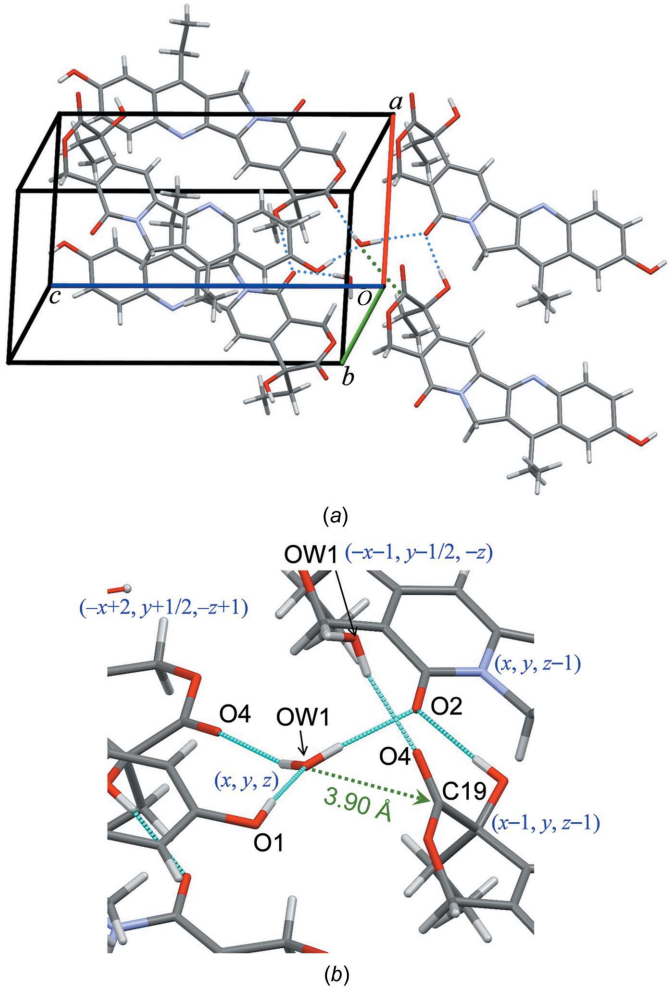

Figure 3
(*a*) The crystal packing of SN-38 monohydrate. Hydrogen bonds are shown as blue dotted lines. The O atom of the water molecule and a carbonyl C atom in the lactone ring nearest to the water molecule are connected with a green dotted line. (*b*) The hydrogen-bond network around the water molecule.

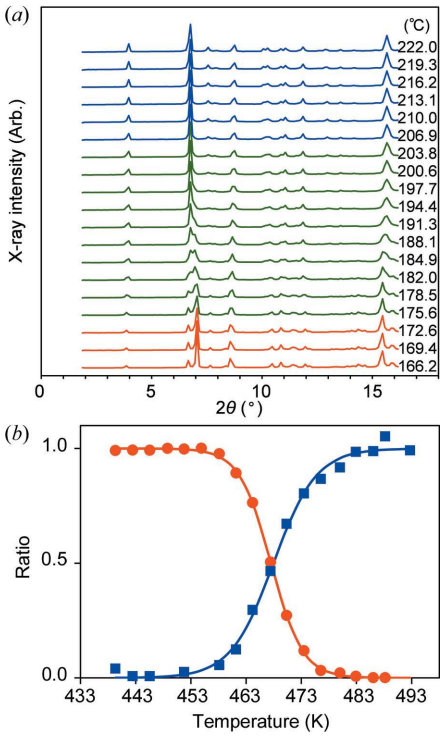

Figure 4
(*a*) PXRD profiles of SN-38 monohydrate on heating. Enlarged profiles around 10.1° are shown in supplementary Fig. S1. (*b*) Changes in the diffraction intensity on heating. $I(T)/I_{max}$ values are plotted as a function of temperature T for the ($\bar{1}$01) diffraction peak of the SN-38 monohydrate crystal (red) and that at a 2θ value of around 10.1° (blue). The equation for a sigmoidal curve, $I(T)/I_{max} = \{1 + \exp[-k(T - C)]\}^{-1} + A$, was fitted to the plots using a non-linear least-squares method to determine the parameters A, C and k (Watanabe *et al.*, 2016), shown as red and blue solid lines.

the *b*-axis direction (Fig. 3*a*). Four hydrogen bonds are found in the crystal structure: one between neighbouring SN-38 molecules, and the rest between SN-38 and water molecules (Table 2). The hydrogen bond between the O5—H group at (x, y, z) and atom O2 at ($x + 1$, y, z) links the SN-38 molecules along the *a* axis.

When the SN-38·H_2O crystals were heated, the intensities of the diffraction peaks of the SN-38·H_2O crystals began to decrease at 453 K and became almost zero at around 480 K (Fig. 4*a*). Instead, new diffraction peaks emerged at 453 K and their diffraction intensities reached a constant value beyond 480 K. The temperature at which the intensities of the ($\bar{1}$01) peaks halved was 467 K, as calculated using a fitted sigmoidal curve (Fig. 4*b*). These changes in the PXRD profiles indicate that the SN-38 monohydrate crystal is transformed into another crystal form by heating. Cell parameters regarding the peaks found in the PXRD profiles above 478 K could not be determined using *EXPO2014* (Altomare *et al.*, 2013), probably because the sample was a mixture of polymorphs and degradation products of SN-38. HPLC analyses of the SN-38·H_2O crystals that were heated to 473 K for 10 min revealed that the sample consisted of intact SN-38 (60%), the carboxylate form of SN-38 (30%) and unknown compounds (10%). This indicates that 60% of SN-38 was transformed into another polymorph, possibly an anhydrate form, while 30% was hydrolysed and 10% was degraded as a result of heating. The sum of the ratios in Fig. 4(*b*) was almost 1 during the heating process, suggesting that the proportion of SN-38 monohydrate decreased and the compound relating to the reflection around 10.1° emerged simultaneously.

Table 2
Hydrogen-bond geometry (Å, °).

D—H···A	D—H	H···A	D···A	D—H···A
O1—H1···*OW*1	0.84	1.91	2.732 (3)	168
O5—H5···O2^{i}	0.84	2.06	2.896 (3)	173
*OW*1—H*W*1*A*···O2^{ii}	0.85 (1)	2.07 (2)	2.881 (3)	160 (4)
*OW*1—H*W*1*B*···O4^{iii}	0.84 (1)	2.13 (2)	2.894 (3)	152 (4)

Symmetry codes: (i) $x, y, z + 1$; (ii) $x - 1, y, z$; (iii) $-x + 1, y - \frac{1}{2}, -z + 2$.

In the crystal structure of (I), the O atom of the water molecule, O*W*1, is located at a distance of 3.897 (3) Å from the carbonyl C19 atom of the lactone ring at ($x - 1$, y, $z - 1$), and the angle formed by the O*W*1···C19 line and the best-fit plane of the carbonyl group of the lactone is 54.9°. This suggests that the water molecule can get close to atom C19 at ($x - 1$, y, $z - 1$) in the crystal structure. The O4 atom of the lactone ring at ($x - 1$, y, $z - 1$) is hydrogen bonded as a hydrogen-bond acceptor to the water molecule at ($-x - 1$, $y - \frac{1}{2}$, $-z$). These molecular arrangements in the crystal structure imply that the

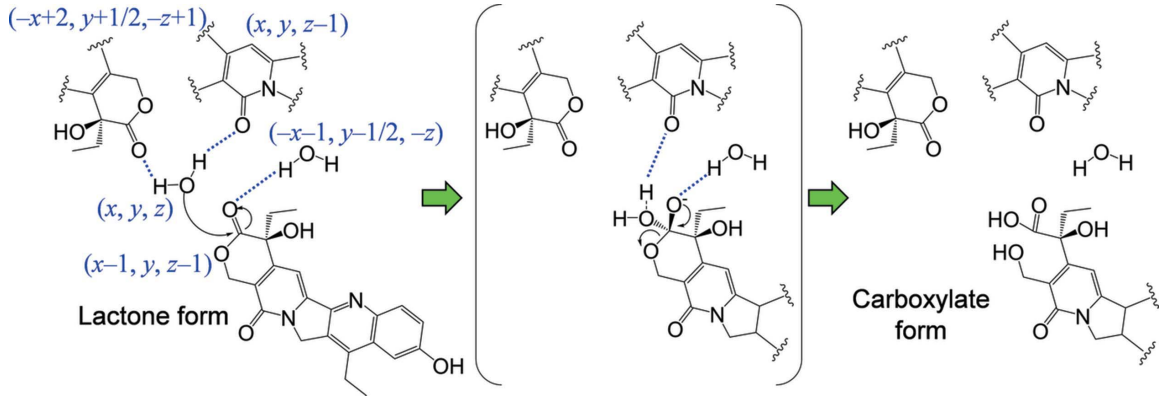

Figure 5
A possible mechanism for the hydrolytic degradation of SN-38 in the crystal on heating.

lactone ring of SN-38 may become hydrolysed, as shown in Fig. 5.

First, the water molecule at (x, y, z) would nucleophilically attack the carbonyl C19 atom at $(x-1, y, z-1)$. The hydrogen bond between atom H*W*1*A* of the water molecule and the carbonyl O2 atom at $(x, y, z-1)$ would enhance the nucleophilicity of the water molecule as a general base, while the hydrogen bond between the carbonyl O4 atom at $(x-1, y, z-1)$ as a hydrogen-bond acceptor and the water molecule at $(-x-1, y-\frac{1}{2}, -z)$ would enhance the electrophilicity of C19. A tetrahedral intermediate would then be formed by the nucleophilic attack of the water molecule, and the intermediate might also be stabilized through these hydrogen bonds. Atom O3 in the tetrahedral intermediate would leave C19, finally resulting in the formation of the carboxylate form of SN-38. Once the carboxylate form has formed, the molecular arrangement conducive to hydrolysis of the lactone ring may be disturbed in the crystal structure, which may partly explain why not all SN-38 molecules in the crystal were hydrolysed on heating.

These heat-labile characteristics of SN-38 monohydrate suggest that heating processes should be carefully avoided in the manufacture of formulations containing the monohydrate.

Acknowledgements

MAA thanks The Uehara Memorial Foundation for a research fellowship. The synchrotron radiation experiment on BL02B1 was performed with the approval of the Japan Synchrotron Radiation Research Institute (JASRI proposal No. 2015 A1293). The synchrotron radiation experiment on BL5S2 was performed with the approval of the Aichi Synchrotron Radiation Center, Aichi Science and Technology Foundation, Aichi, Japan (proposal No. 201503006). This work was supported by the Japan Society for the Promotion of Science KAKENHI (grant Nos. 26460224, 26460039 and 26460226).

References

Ali, M. A., Noguchi, S., Iwao, Y., Oka, T. & Itai, S. (2016). *Chem. Pharm. Bull.* **64**, 577–584.
Altomare, A., Cuocci, C., Giacovazzo, C., Moliterni, A., Rizzi, R., Corriero, N. & Falcicchio, A. (2013). *J. Appl. Cryst.* **46**, 1231–1235.
Chabot, G. G. (1997). *Clin. Pharmacokinet.* **33**, 245–259.
Dai, N., Jenkinson, S. F., Fleet, G. W. J. & Watkin, D. J. (2010). *Acta Cryst.* E**66**, o406–o407.
Groom, C. R. & Allen, F. H. (2014). *Angew. Chem. Int. Ed.* **53**, 662–671.
Hamaguchi, T., Doi, T., Eguchi-Nakajima, T., Kato, K., Yamada, Y., Shimada, Y., Fuse, N., Ohtsu, A., Matsumoto, S., Takanashi, M. & Matsumura, Y. (2010). *Clin. Cancer Res.* **16**, 5058–5066.
Hübschle, C. B., Sheldrick, G. M. & Dittrich, B. (2011). *J. Appl. Cryst.* **44**, 1281–1284.
Jenkinson, S. F., Dai, N., Fleet, G. W. J. & Watkin, D. J. (2010). *Acta Cryst.* E**66**, o1221–o1222.
Kolhatkar, R. B., Swaan, P. & Ghandehari, H. (2008). *Pharm. Res.* **25**, 1723–1729.
Latinen, I. (2006). US Patent US7910737 B2.
Macrae, C. F., Bruno, I. J., Chisholm, J. A., Edgington, P. R., McCabe, P., Pidcock, E., Rodriguez-Monge, L., Taylor, R., van de Streek, J. & Wood, P. A. (2008). *J. Appl. Cryst.* **41**, 466–470.
McPhail, A. T. & Sim, G. A. (1968). *J. Chem. Soc. B*, pp. 923–928.
Pommier, Y. (2006). *Nat. Rev. Cancer*, **6**, 789–802.
Potmesil, M. (1994). *Cancer Res.* **54**, 1431–1439.
Rigaku (1999). *RAPID-AUTO*. Rigaku Corporation, Tokyo, Japan.
Rothenberg, M. L., Kuhn, J. G., Schaaf, L. J., Rodriguez, G. I., Eckhardt, S. G., Villalona-Calero, M. A., Rinaldi, D. A., Hammond, L. A., Hodges, S., Sharma, A., Elfring, G. L., Petit, R. G., Locker, P. K., Miller, L. L. & von Hoff, D. D. (2001). *Ann. Oncol.* **12**, 1631–1641.
Sapra, P., Zhao, H., Mehlig, M., Malaby, J., Kraft, P., Longley, C., Greenberger, L. M. & Horak, I. D. (2008). *Clin. Cancer Res.* **14**, 1888–1896.
Sawada, S., Okajima, S., Aiyama, R., Nokata, K., Furuta, T., Yokokura, T., Sugino, E., Yamaguchi, K. & Miyasaka, T. (1991). *Chem. Pharm. Bull.* **39**, 1446–1450.
Sepehri, N., Rouhani, H., Tavassolian, F., Montazeri, H., Khoshayand, M. R., Ghahremani, M. H., Ostad, S. N., Atyabi, F. & Dinarvand, R. (2014). *Int. J. Pharm.* **471**, 485–497.
Sheldrick, G. M. (2015*a*). *Acta Cryst.* A**71**, 3–8.
Sheldrick, G. M. (2015*b*). *Acta Cryst.* C**71**, 3–8.
Thakur, R., Sivakumar, B. & Savva, M. (2010). *J. Phys. Chem. B*, **114**, 5903–5911.
Wang, H. K., Lin, S. Y., Hwang, K. M., McPhail, A. T. & Lee, K. H. (1995). *Bioorg. Med. Chem. Lett.* **5**, 77–82.
Watanabe, M., Mizoguchi, M., Aoki, H., Iwao, Y., Noguchi, S. & Itai, S. (2016). *Int. J. Pharm.* **512**, 108–117.
Westrip, S. P. (2010). *J. Appl. Cryst.* **43**, 920–925.
Zhang, J. A., Xuan, T., Parmar, M., Ma, L., Ugwu, S., Ali, S. & Ahmad, I. (2004). *Int. J. Pharm.* **270**, 93–107.

supporting information

Acta Cryst. (2016). C**72**, 743-747 [doi:10.1107/S2053229616014492]

The antitumour drug 7-ethyl-10-hydroxycamptothecin monohydrate and its solid-state hydrolysis mechanism on heating

Md. Ashraf Ali, Shuji Noguchi, Miteki Watanabe, Yasunori Iwao and Shigeru Itai

Computing details

Data collection: *RAPID-AUTO* (Rigaku, 1999); cell refinement: *RAPID-AUTO* (Rigaku, 1999); data reduction: *RAPID-AUTO* (Rigaku, 1999); program(s) used to solve structure: *SHELXT* (Sheldrick, 2015*a*); program(s) used to refine structure: *SHELXL2014*/7 (Sheldrick, 2015*b*), *SHELXLE* (Hübschle *et al.*, 2011); molecular graphics: *Mercury* (Macrae *et al.*, 2008); software used to prepare material for publication: *publCIF* (Westrip, 2010).

(4S)-4,11-Diethyl-4,9-dihydroxy-1H-pyrano[3′,4′:6,7] indolizino[1,2-b]quinoline-3,14(4H,12H)dione

Crystal data

$C_{22}H_{20}N_2O_5·H_2O$
M_r = 410.41
Monoclinic, $P2_1$
a = 8.529 (2) Å
b = 7.352 (2) Å
c = 15.075 (3) Å
β = 100.18 (3)°
V = 930.3 (4) Å^3
Z = 2
$F(000)$ = 432
D_x = 1.465 Mg m^{-3}
Synchrotron (SPring-8 BL02B1) radiation, λ = 0.70041 Å
Cell parameters from 255 reflections
θ = 1.2–6.7°
μ = 0.11 mm^{-1}
T = 100 K
Column, pale yellow
0.20 × 0.01 × 0.01 mm

Data collection

Rigaku Mercury2 four-circle diffractometer with CCD area detector
Radiation source: synchrotron
ω scan
13173 measured reflections
4345 independent reflections
3684 reflections with $I > 2\sigma(I)$
R_{int} = 0.056
θ_{max} = 28.7°, θ_{min} = 1.4°
h = −11→8
k = −6→9
l = −20→20

Refinement

Refinement on F^2
Least-squares matrix: full
$R[F^2 > 2\sigma(F^2)]$ = 0.043
$wR(F^2)$ = 0.120
S = 0.84
4345 reflections
281 parameters
16 restraints
Primary atom site location: structure-invariant direct methods
Secondary atom site location: difference Fourier map
Hydrogen site location: mixed
H atoms treated by a mixture of independent and constrained refinement
$w = 1/[\sigma^2(F_o^2) + (0.1P)^2]$ where $P = (F_o^2 + 2F_c^2)/3$
$(\Delta/\sigma)_{max} < 0.001$
$\Delta\rho_{max}$ = 0.42 e Å^{-3}
$\Delta\rho_{min}$ = −0.28 e Å^{-3}

Special details

Geometry. All esds (except the esd in the dihedral angle between two l.s. planes) are estimated using the full covariance matrix. The cell esds are taken into account individually in the estimation of esds in distances, angles and torsion angles; correlations between esds in cell parameters are only used when they are defined by crystal symmetry. An approximate (isotropic) treatment of cell esds is used for estimating esds involving l.s. planes.

Fractional atomic coordinates and isotropic or equivalent isotropic displacement parameters (Å²)

	x	*y*	*z*	U_{iso}*/U_{eq}
O1	0.3063 (2)	0.4942 (3)	0.14614 (11)	0.0191 (5)
H1	0.3636	0.4929	0.1062	0.023*
N1	0.6918 (2)	0.4835 (3)	0.48097 (12)	0.0109 (4)
C1	0.4001 (3)	0.4971 (4)	0.22858 (15)	0.0136 (5)
O2	0.5040 (2)	0.4379 (3)	0.83245 (11)	0.0148 (4)
N2	0.5875 (2)	0.4670 (3)	0.69791 (12)	0.0101 (4)
C2	0.5673 (3)	0.4941 (5)	0.23798 (15)	0.0159 (6)
H2	0.6159	0.4925	0.1859	0.019*
C3	0.6596 (3)	0.4934 (4)	0.32162 (15)	0.0138 (5)
H3	0.7723	0.4927	0.3272	0.017*
O3	0.9750 (2)	0.2875 (3)	0.94861 (12)	0.0178 (4)
C4	0.5905 (3)	0.4938 (4)	0.40030 (14)	0.0109 (5)
O4	1.2123 (2)	0.2186 (3)	0.92289 (13)	0.0216 (5)
C5	0.4212 (3)	0.5057 (4)	0.39111 (14)	0.0099 (5)
O5	1.1680 (2)	0.3924 (3)	0.76177 (11)	0.0150 (5)
H5	1.2640	0.4005	0.7866	0.018*
OW1	0.4846 (2)	0.5435 (4)	0.01413 (13)	0.0259 (6)
HW1A	0.488 (4)	0.500 (5)	−0.0369 (14)	0.031*
HW1B	0.562 (3)	0.614 (5)	0.027 (2)	0.031*
C6	0.3287 (3)	0.5077 (4)	0.30356 (15)	0.0128 (5)
H6	0.2160	0.5165	0.2963	0.015*
C21	1.1135 (3)	0.6280 (4)	0.86604 (17)	0.0157 (6)
H21A	1.0606	0.6433	0.9190	0.019*
H21B	1.2300	0.6325	0.8877	0.019*
C20	0.8278 (3)	0.3921 (4)	0.92659 (16)	0.0146 (6)
H20A	0.8416	0.5105	0.9583	0.018*
H20B	0.7408	0.3256	0.9481	0.018*
C19	1.0918 (3)	0.3042 (4)	0.90154 (16)	0.0146 (6)
C18	1.0696 (3)	0.4405 (4)	0.82395 (14)	0.0117 (5)
C17	0.6166 (3)	0.4422 (4)	0.78970 (15)	0.0105 (5)
C16	0.7825 (3)	0.4245 (4)	0.82765 (15)	0.0117 (5)
C15	0.8984 (3)	0.4369 (4)	0.77579 (15)	0.0102 (5)
C14	0.8595 (3)	0.4540 (4)	0.68131 (14)	0.0111 (5)
H14	0.9396	0.4564	0.6448	0.013*
C13	0.7028 (3)	0.4669 (4)	0.64496 (14)	0.0106 (5)
C12	0.4254 (3)	0.4900 (4)	0.64572 (14)	0.0115 (5)
H12A	0.3755	0.6036	0.6625	0.014*
H12B	0.3564	0.3854	0.6541	0.014*
C11	0.6212 (3)	0.4838 (4)	0.55175 (14)	0.0098 (5)

C10	0.4570 (3)	0.4985 (4)	0.55105 (15)	0.0108 (5)
C7	0.3531 (3)	0.5150 (4)	0.47127 (15)	0.0100 (5)
C8	0.1777 (3)	0.5392 (4)	0.46971 (16)	0.0128 (5)
H8A	0.1328	0.6163	0.4175	0.015*
H8B	0.1623	0.6039	0.5251	0.015*
C22	1.0666 (4)	0.7842 (5)	0.8020 (2)	0.0258 (7)
H22A	0.9502	0.7935	0.7882	0.031*
H22B	1.1080	0.7631	0.7462	0.031*
H22C	1.1112	0.8976	0.8300	0.031*
C9	0.0871 (3)	0.3616 (5)	0.4636 (2)	0.0206 (6)
H9A	−0.0263	0.3862	0.4619	0.025*
H9B	0.1280	0.2863	0.5162	0.025*
H9C	0.1010	0.2971	0.4086	0.025*

Atomic displacement parameters (Å²)

	U^{11}	U^{22}	U^{33}	U^{12}	U^{13}	U^{23}
O1	0.0172 (8)	0.0388 (14)	0.0013 (7)	0.0003 (10)	0.0016 (6)	0.0001 (8)
N1	0.0113 (8)	0.0186 (13)	0.0034 (8)	−0.0004 (9)	0.0030 (7)	0.0013 (8)
C1	0.0161 (11)	0.0200 (15)	0.0045 (10)	−0.0002 (11)	0.0010 (8)	0.0010 (10)
O2	0.0136 (8)	0.0293 (12)	0.0031 (7)	−0.0004 (8)	0.0059 (6)	−0.0008 (7)
N2	0.0091 (8)	0.0187 (13)	0.0032 (8)	0.0007 (9)	0.0031 (6)	−0.0004 (8)
C2	0.0176 (11)	0.0268 (17)	0.0048 (9)	0.0008 (12)	0.0061 (8)	0.0002 (10)
C3	0.0118 (10)	0.0246 (16)	0.0062 (9)	0.0001 (11)	0.0048 (8)	0.0016 (10)
O3	0.0151 (8)	0.0331 (13)	0.0062 (7)	0.0032 (8)	0.0047 (6)	0.0080 (8)
C4	0.0124 (10)	0.0173 (15)	0.0035 (9)	−0.0005 (11)	0.0028 (8)	0.0008 (9)
O4	0.0191 (10)	0.0324 (14)	0.0143 (9)	0.0067 (9)	0.0052 (7)	0.0084 (8)
C5	0.0112 (10)	0.0149 (14)	0.0042 (9)	0.0000 (10)	0.0028 (7)	0.0011 (9)
O5	0.0085 (8)	0.0340 (14)	0.0039 (7)	0.0037 (8)	0.0048 (6)	−0.0018 (7)
OW1	0.0227 (10)	0.0524 (17)	0.0046 (8)	−0.0111 (10)	0.0075 (7)	−0.0076 (9)
C6	0.0117 (10)	0.0206 (15)	0.0058 (10)	−0.0007 (11)	0.0010 (8)	0.0001 (10)
C21	0.0153 (12)	0.0241 (16)	0.0080 (10)	−0.0014 (11)	0.0028 (9)	−0.0026 (10)
C20	0.0133 (11)	0.0270 (18)	0.0045 (10)	0.0018 (11)	0.0039 (8)	0.0009 (10)
C19	0.0152 (12)	0.0233 (16)	0.0055 (10)	−0.0002 (11)	0.0023 (9)	0.0001 (10)
C18	0.0102 (10)	0.0237 (15)	0.0024 (9)	0.0009 (10)	0.0044 (7)	0.0003 (9)
C17	0.0124 (10)	0.0166 (14)	0.0035 (9)	−0.0004 (10)	0.0042 (8)	−0.0007 (9)
C16	0.0126 (10)	0.0202 (15)	0.0029 (9)	0.0000 (10)	0.0034 (8)	0.0005 (9)
C15	0.0116 (10)	0.0146 (14)	0.0047 (9)	0.0010 (10)	0.0026 (8)	0.0011 (9)
C14	0.0123 (10)	0.0185 (15)	0.0037 (9)	−0.0005 (10)	0.0046 (8)	−0.0001 (9)
C13	0.0127 (10)	0.0169 (15)	0.0035 (9)	−0.0009 (10)	0.0048 (7)	0.0004 (9)
C12	0.0097 (9)	0.0230 (16)	0.0024 (9)	0.0014 (11)	0.0030 (7)	−0.0004 (10)
C11	0.0099 (9)	0.0157 (14)	0.0040 (9)	0.0003 (10)	0.0021 (7)	0.0008 (9)
C10	0.0129 (10)	0.0160 (14)	0.0046 (9)	−0.0011 (11)	0.0045 (8)	0.0001 (9)
C7	0.0112 (10)	0.0138 (14)	0.0059 (10)	−0.0010 (10)	0.0040 (8)	0.0006 (9)
C8	0.0111 (11)	0.0203 (16)	0.0073 (10)	0.0029 (10)	0.0029 (8)	−0.0002 (9)
C22	0.0238 (14)	0.0229 (18)	0.0296 (16)	−0.0054 (13)	0.0013 (12)	0.0025 (13)
C9	0.0123 (12)	0.0255 (18)	0.0243 (14)	−0.0011 (11)	0.0048 (10)	0.0016 (12)

Geometric parameters (Å, º)

O1—C1	1.354 (3)	C21—H21B	0.9900
O1—H1	0.8400	C20—C16	1.492 (3)
N1—C11	1.315 (3)	C20—H20A	0.9900
N1—C4	1.364 (3)	C20—H20B	0.9900
C1—C6	1.378 (3)	C19—C18	1.526 (4)
C1—C2	1.408 (3)	C18—C15	1.511 (3)
O2—C17	1.248 (3)	C17—C16	1.435 (3)
N2—C13	1.372 (3)	C16—C15	1.368 (3)
N2—C17	1.374 (3)	C15—C14	1.410 (3)
N2—C12	1.475 (3)	C14—C13	1.356 (3)
C2—C3	1.363 (3)	C14—H14	0.9500
C2—H2	0.9500	C13—C11	1.459 (3)
C3—C4	1.415 (3)	C12—C10	1.500 (3)
C3—H3	0.9500	C12—H12A	0.9900
O3—C19	1.327 (3)	C12—H12B	0.9900
O3—C20	1.460 (3)	C11—C10	1.403 (3)
C4—C5	1.428 (3)	C10—C7	1.367 (3)
O4—C19	1.200 (3)	C7—C8	1.502 (3)
C5—C6	1.413 (3)	C8—C9	1.511 (4)
C5—C7	1.432 (3)	C8—H8A	0.9900
O5—C18	1.409 (3)	C8—H8B	0.9900
O5—H5	0.8400	C22—H22A	0.9800
OW1—HW1A	0.839 (13)	C22—H22B	0.9800
OW1—HW1B	0.836 (13)	C22—H22C	0.9800
C6—H6	0.9500	C9—H9A	0.9800
C21—C22	1.508 (4)	C9—H9B	0.9800
C21—C18	1.536 (4)	C9—H9C	0.9800
C21—H21A	0.9900		

C1—O1—H1	109.5	O2—C17—C16	125.9 (2)
C11—N1—C4	114.48 (18)	N2—C17—C16	113.8 (2)
O1—C1—C6	118.6 (2)	C15—C16—C17	121.8 (2)
O1—C1—C2	121.0 (2)	C15—C16—C20	119.7 (2)
C6—C1—C2	120.3 (2)	C17—C16—C20	118.4 (2)
C13—N2—C17	124.44 (19)	C16—C15—C14	121.2 (2)
C13—N2—C12	112.99 (18)	C16—C15—C18	117.46 (19)
C17—N2—C12	122.53 (19)	C14—C15—C18	121.2 (2)
C3—C2—C1	120.1 (2)	C13—C14—C15	117.0 (2)
C3—C2—H2	119.9	C13—C14—H14	121.5
C1—C2—H2	119.9	C15—C14—H14	121.5
C2—C3—C4	121.2 (2)	C14—C13—N2	121.5 (2)
C2—C3—H3	119.4	C14—C13—C11	131.6 (2)
C4—C3—H3	119.4	N2—C13—C11	106.93 (18)
C19—O3—C20	121.8 (2)	N2—C12—C10	101.73 (17)
N1—C4—C3	117.1 (2)	N2—C12—H12A	111.4
N1—C4—C5	124.07 (19)	C10—C12—H12A	111.4

C3—C4—C5	118.9 (2)	N2—C12—H12B	111.4
C6—C5—C4	118.62 (19)	C10—C12—H12B	111.4
C6—C5—C7	123.0 (2)	H12A—C12—H12B	109.3
C4—C5—C7	118.36 (19)	N1—C11—C10	126.5 (2)
C18—O5—H5	109.5	N1—C11—C13	124.9 (2)
HW1A—OW1—HW1B	107 (2)	C10—C11—C13	108.63 (19)
C1—C6—C5	120.7 (2)	C7—C10—C11	120.3 (2)
C1—C6—H6	119.6	C7—C10—C12	130.0 (2)
C5—C6—H6	119.6	C11—C10—C12	109.68 (19)
C22—C21—C18	113.7 (2)	C10—C7—C5	116.2 (2)
C22—C21—H21A	108.8	C10—C7—C8	120.8 (2)
C18—C21—H21A	108.8	C5—C7—C8	122.9 (2)
C22—C21—H21B	108.8	C7—C8—C9	113.3 (2)
C18—C21—H21B	108.8	C7—C8—H8A	108.9
H21A—C21—H21B	107.7	C9—C8—H8A	108.9
O3—C20—C16	111.8 (2)	C7—C8—H8B	108.9
O3—C20—H20A	109.3	C9—C8—H8B	108.9
C16—C20—H20A	109.3	H8A—C8—H8B	107.7
O3—C20—H20B	109.3	C21—C22—H22A	109.5
C16—C20—H20B	109.3	C21—C22—H22B	109.5
H20A—C20—H20B	107.9	H22A—C22—H22B	109.5
O4—C19—O3	119.8 (2)	C21—C22—H22C	109.5
O4—C19—C18	122.3 (2)	H22A—C22—H22C	109.5
O3—C19—C18	117.8 (2)	H22B—C22—H22C	109.5
O5—C18—C15	108.33 (18)	C8—C9—H9A	109.5
O5—C18—C19	109.7 (2)	C8—C9—H9B	109.5
C15—C18—C19	109.6 (2)	H9A—C9—H9B	109.5
O5—C18—C21	111.7 (2)	C8—C9—H9C	109.5
C15—C18—C21	111.0 (2)	H9A—C9—H9C	109.5
C19—C18—C21	106.5 (2)	H9B—C9—H9C	109.5
O2—C17—N2	120.3 (2)		

Hydrogen-bond geometry (Å, º)

D—H···*A*	*D*—H	H···*A*	*D*···*A*	*D*—H···*A*
O1—H1···O*W*1	0.84	1.91	2.734 (3)	168
O5—H5···O2^{i}	0.84	2.06	2.894 (3)	172
O*W*1—H*W*1*A*···O2^{ii}	0.84 (1)	2.05 (2)	2.879 (3)	170 (4)
O*W*1—H*W*1*B*···O4^{iii}	0.84 (1)	2.09 (2)	2.894 (3)	162 (4)

Symmetry codes: (i) *x*+1, *y*, *z*; (ii) *x*, *y*, *z*−1; (iii) −*x*+2, *y*+1/2, −*z*+1.